

# Adversarially Trained Model Compression: When Robustness Meets Efficiency

Shupeng Gui  
University of Rochester  
sgui2@ur.rochester.edu

Haotao Wang  
Texas A&M University  
htwang@tamu.edu

Chen Yu  
University of Rochester  
cyu28@ur.rochester.edu

Haichuan Yang  
University of Rochester  
h.yang@rochester.edu

Zhangyang Wang  
Texas A&M University  
atlaswang@tamu.edu

Ji Liu  
University of Rochester  
ji.liu.uwisc@gmail.com

December 1, 2021

## Abstract

The robustness of deep models to adversarial attacks has gained significant attention in recent years, so has the model compactness and efficiency: yet the two have been mostly studied separately, with few relationships drawn between each other. This paper is concerned with: how can we combine the best of both worlds, obtaining a **robust and compact** network? The answer is not as straightforward as it may seem, since the two goals of model robustness and compactness may contradict from time to time. We formally study this new question, by proposing a novel *Adversarially Trained Model Compression (ATMC)* framework. A unified constrained optimization formulation is designed, with an efficient algorithm developed. An extensive group of experiments are then carefully designed and presented, demonstrating that ATMC obtains remarkably more favorable trade-off among model size, accuracy and robustness, over currently available alternatives in various settings.

## 1 Introduction

As more Internet-of-Things (IoT) devices come online, they are equipped with the ability to ingest and analyze information from their ambient environments via sensor inputs. Over the past few years, convolutional neural networks (CNNs) have led to rapid advances in the predictive performance, that approach and sometimes exceed human performance in a large variety of tasks [Deng et al., 2009]. It is appealing to deploy CNNs onto IoT devices to interpret multimedia big data and intelligently react to both user and environmental events. However, the **efficiency** of typical CNN models (e.g., size, inference speed, and energy cost) becomes a critical hurdle. Their often prohibitive complexity remains a major inhibitor for their more extensive applications in IoT systems, that are often resource-constrained and latency-sensitive. Therefore, CNN model compression [Cheng et al., 2017] is becoming an increasingly demanded technique and has been extensively studied [Liu et al., 2015, Zhou et al., 2016, Li et al., 2016].

On a separate note, the prevailing deployment of CNNs also calls for attention to their **robustness**. Despite their impressive predictive powers, the state-of-the-art CNNs remain to commonly suffer from fragility to adversarial attacks, i.e., a well-trained CNN-based image classifier could be easily fooled to make unreasonably wrong predictions, by perturbing the input image with a small, often unnoticeable variation [Athalye et al., 2018, Carlini and Wagner, 2017, Goodfellow et al., 2014, Kurakin et al., 2016, Luo et al., 2018, Madry et al., 2017, Moosavi-Dezfooli et al., 2016, Xie et al., 2017]. Other tasks, such as 3D mesh classification [Athalye and Sutskever, 2017], image segmentation [Hendrik Metzen et al., 2017], and graph classification [Zügner et al., 2018], were all shown to be vulnerable to adversarial attacks. Apparently, such findings put CNN models in jeopardy for security- and trust-sensitive IoT applications, such as bio-metric verification on mobile devices. Correspondingly, many defense methods are also developed to enhance CNN robustness to adversarial attacks [Kurakin et al., 2016, Madry et al., 2017, Sinha et al., 2017].

## 1.1 Related work

**Improving CNN Robustness by Defenses** There are a magnitude of adversarial defense methods proposed, ranging from hiding gradients [Tramér et al., 2017], to adding stochasticity [Dhillon et al., 2018], to label smoothening/defensive distillation [Papernot and McDaniel, 2017, Papernot et al., 2016], to feature squeezing [Xu et al., 2017], among many more [Hosseini et al., 2017, Meng and Chen, 2017, Liao et al., 2018]. A handful of recent works pointed out that those empirical defenses could still be easily compromised [Athalye et al., 2018], and a few provable defenses were introduced [Madry et al., 2017, Sinha et al., 2017].

**Improving CNN Efficiency by Compression** CNN compression is an extensively studied field for reducing models sizes and speeding up inference. We review three representative mainstreams of compression methods: weight pruning, weight matrix factorization, and quantization.

Pruning refers to sparsifying the model by zeroing out non-significant weights, e.g., by thresholding the weights magnitudes [Han et al., 2015b]. Later on, various forms of sparsity regularization were explicitly incorporated in the training process [Liu et al., 2015, Zhou et al., 2016]. More structured sparsity was also introduced such as through channel pruning [Li et al., 2016, Wen et al., 2016].

Most convolutional and fully-connected layers consist of large tensors to store their parameters [Denton et al., 2014, Jin et al., 2014, Nakkiran et al., 2015], in which there is large redundancy due to the highly-structured filters or columns [Denton et al., 2014, Jin et al., 2014, Nakkiran et al., 2015]. Low-rank factorization was thus adopted to (approximately) decompose large weight matrices into several much smaller matrix factors [Lebedev et al., 2014, Denton et al., 2014, Tai et al., 2015]. The combination of low-rank factorization and pruning/sparsification has shown further effectiveness [Yu et al., 2017].

Quantization saves model size and computation by reducing float-number elements to lower numerical precision, e.g., from 32 bits to 8 bits or less [Wu et al., 2016, Han et al., 2015a]. The model could even consist of only binary weights in the extreme case [Courbariaux et al., 2015, Rastegari et al., 2016]. Beyond scalar quantization, vector quantization was also widely adopted in compression for parameter sharing [Gong et al., 2014, Wu et al., 2018].

**Connecting Robustness to Efficiency** To our best knowledge, there have been few existing studies on relating a CNN model's efficiency and its robustness. A latest work [Guo et al., 2018] demonstrated a complicated intrinsic relationship between CNN weight sparsity and adversarial robustness. The authors reported that an appropriately higher model sparsity implied better robustness, whereas over-sparsification (e.g., less than 5% non-zero parameters) could lead to more fragility. Although model sparsification (i.e., pruning) is only one specific case of CNN compression, their observation is inspiring.

## 1.2 Our Contribution

As far as we know, this paper describes the first attempt to jointly optimize the two key goals: CNN robustness to adversarial attacks, and efficiency/compactness. We propose a unified constrained optimization framework for compressing large-scale CNNs into both robust and compact models. The framework, dubbed *adversarially trained model compression (ATMC)*, features a seamless integration of adversarial training (formulated as the optimization objective), and structured weight decomposition/sparsification (formulated as the constraint). An efficient algorithm is derived to solve this challenging constrained problem.

We then conduct an extensive set of experiments, comparing ATMC with various baselines and off-the-shelf solutions. ATMC consistently shows significant advantages in achieving the most competitive robustness-model size trade-offs. As an interesting observation, the models compressed by ATMC can achieve very high compression ratios, while still maintaining considerable robustness, manifesting the value of jointly optimizing the two goals in one framework, under which they mutually benefit.

## 2 Adversarially Trained Model Compression

In this section, we define and solve the ATMC problem. ATMC is formulated as a constrained min-max optimization problem: the adversarial training makes the min-max objective (Section 2.1), while the model compression by enforcing certain weight structures constitutes the constraint (Section 2.2). We then derive the algorithm to solve the ATMC formulation (Section 2.3).

### 2.1 Formulating the ATMC Objective: Adversarial Robustness

We consider a common white-box attack setting [Kurakin et al., 2016]. The white box attack allows an adversary to eavesdrop the optimization and gradients of the learning model. Each time, when an “clean” image  $x$  comes to a target model, the attacker is allowed to “perturb” the image into  $x'$  with an adversarial perturbation with bounded magnitudes. Specifically, let  $\rho \geq 0$  denote the predefined bound for the attack magnitude,  $x'$  must be from the following set:

$$B_{\infty}^{\rho}(x) := \{x' : \|x' - x\|_{\infty} \leq \rho\}.$$

The objective for the attacker is to perturb  $X'$  within  $B_{\infty}^{\rho}(x)$ , such as the target model performance is maximally deteriorated. Formally, let  $f(x, y; \theta)$  be the loss function that the target model aims to minimize, where  $\theta$  denotes the model parameters and  $(x, y)$  the training pairs. The adversarial loss, i.e., the training objective for the attacker, is defined by

$$f^{\text{adv}}(\theta; x, y) = \max_{x' \in B_{\infty}^{\rho}(x)} f(\theta; x', y) \quad (1)$$

It could be understood that the maximum (worst) target model loss attainable at any point within  $B_{\infty}^{\rho}(x)$ . Next, since the target model needs to defend against the attacker, it requires to suppress the worst risk. Therefore, the overall objective for the target model to gain adversarial robustness could be expressed as  $\mathcal{Z}$  denotes the training data set:

$$\min_{\theta} \sum_{(x,y) \in \mathcal{Z}} f^{\text{adv}}(\theta; x, y). \quad (2)$$

## 2.2 Formulating the ATMC Constraint: Structured Compression

As we reviewed previously, typical CNN model compression strategies include pruning (element-level [Han et al., 2015b], or channel-level [Li et al., 2016]), low-rank factorization [Lebedev et al., 2014, Denton et al., 2014, Tai et al., 2015], and quantization [Gong et al., 2014, Wu et al., 2016, Han et al., 2015a]. In this work, we focus on incorporating pruning and factorization methods, to formulate the structured constraint for the desired compact CNN weights. Quantization could be easily incorporated in future too; we also conduct empirical experiments later on to show that ATMC is compatible with quantization.

Without loss of generality, we denote the major operation of a CNN layer (either convolutional or fully-connected) as  $x_{\text{out}} = Wx_{\text{in}}$ ,  $W \in \mathbb{R}^{m \times n}$ ,  $m \geq n$ ; computing the non-linearity (neuron) parts takes minor resources compared to the large-scale matrix-vector multiplication. The element-level pruning [Han et al., 2015b] encourages the elements of  $W$  to be zero. The channel pruning [Li et al., 2016] could be viewed as enforcing rows of  $W$  to be zero, which could be considered as a highly-structured special case of element-level pruning. On the other hand, the factorization-based methods decomposes  $W = W_1W_2$ , where  $W_1 \in \mathbb{R}^{m \times p}$ ,  $W_2 \in \mathbb{R}^{p \times n}$ , and usually  $p \leq m, n$ .

Looking at the two strategy options, we propose to enforce the following structure to  $W$ :

$$W = UV + C, \quad \|U\|_0 + \|V\|_0 + \|C\|_0 \leq k. \quad (3)$$

In other words, we enforce a compound (including both multiplicative and additive) sparsity structure on  $W$ , compared to common plain sparsity structures (directly on the elements of  $W$ ). Decomposing a matrix into sparse factors was studied before [Neyshabur and Panigrahy, 2013], but not in a model compression context; we further allow for a sparse error  $C$  for more flexibility in learning weights, as inspired from robust optimization [Candès et al., 2011].

We could also straightforwardly control the dimension  $p$  of  $U, V$  to simultaneously enforce an explicit low-rank factorization structure on  $W$ . However, in practical implementation, we find that using a small  $k$  will naturally give rise to all-zero rows/columns in  $U/V$ , essentially leading to low-rank factorization. Therefore, we choose  $p = m$  by default, and focus on adjusting  $k$ , as the only hyper-parameter to control the model compression ratio: it simplifies the ATMC model tuning and usage. Also in practice, we regularize  $U$  to be within an  $\ell_0$ -ball of an identity matrix  $I \in \mathbb{R}^{m \times m}$ , as that is found to notably stabilize the optimization.

## 2.3 ATMC: Formulation and Algorithm

Let us use  $\theta$  to denote the (re-parameterized) weights in all  $l$  layers:  $\theta := \{U^{(i)}, V^{(i)}, C^{(i)} : i \in [l]\}$ . We are now ready to present the overall constrained optimization formulation of the proposed ATMC framework:

$$\min_{\theta} \sum_{(x,y) \in \mathcal{Z}} f^{\text{adv}}(\theta; x, y) \quad (4)$$

$$\text{s.t.} \quad \underbrace{\sum_{i=1}^l (\|U^{(i)}\|_0 + \|V^{(i)}\|_0 + \|C^{(i)}\|_0)}_{\|\theta\|_0} \leq k. \quad (5)$$

ATMC needs the only hyperparameter  $k$  to control the compressed model size, i.e., the number of non-zero elements.

We next propose an efficient algorithm to solve equation 4. The original problem is a challenging constrained minimax problem. To simplify it, we could view the “max” part in equation 1 as a new function

$f^{\text{adv}}(\cdot; \cdot)$ , and consider equation 4 as a standard minimization objective, which could be solved using projected stochastic gradient descent (P-SGD). The update formula is as follows:

$$\theta \leftarrow \text{Proj}_{\{\theta' : \|\theta'\|_0 \leq k\}}(\theta - \lambda_t \nabla_{\theta} f^{\text{adv}}(\theta; x, y)).$$

Here,  $\{\theta' : \|\theta'\|_0 \leq k\}$  denotes the feasible domain of  $\theta$  as specified in (5), and  $\lambda_t$  is the learning rate.

**Computing the Gradient** The main bottleneck in the above update formula is to determine the gradient of  $f^{\text{adv}}(\cdot; \cdot)$ , since this function is defined as a maximization in (1). We refer to the following theorem [Danskin, 2012]:

**Theorem 1** (*Danskin’s theorem*) *Let  $g(\mathbf{x}, \mathbf{y})$  ( $\mathbf{x} \in \mathbb{R}^d, \mathbf{y} \in \Omega$  is a compact set) be a differential function in terms of two vector variables  $\mathbf{x}, \mathbf{y}$ . Assume for every  $\mathbf{y} \in \Omega$ ,  $g(\mathbf{x}, \mathbf{y})$  is convex in  $\mathbf{x}$ . Further assume  $G(\mathbf{x}) = \max_{\mathbf{y} \in \Omega} g(\mathbf{x}, \mathbf{y})$  is also a differential function in terms of  $\mathbf{x}$ , and for any  $\mathbf{x}$ , the optimal  $\mathbf{y}^*(\mathbf{x}) = \arg \max_{\mathbf{y} \in \Omega} g(\mathbf{x}, \mathbf{y})$  is unique in  $\Omega$ . Then we have the following result:*

$$\frac{dG(\mathbf{x})}{d\mathbf{x}} = \nabla_{\mathbf{x}} g(\mathbf{x}, \mathbf{y}^*(\mathbf{x})),$$

here  $\nabla_{\mathbf{x}}$  means the partial derivative in terms of the first vector variable of function  $g(\cdot; \cdot)$ .

Based on the Danskin’s theorem, instead of finding  $\nabla_{\theta} f^{\text{adv}}(\theta; x, y)$ , we can first find the “worst adversary”:

$$x^{\text{adv}} = \arg \max_{x' \in B_{\infty}^{\rho}(x)} f(\theta; x', y), \quad (6)$$

and then find  $\nabla_{\theta} f(x^{\text{adv}}, y; \theta)$ , the partial derivative of  $\theta$  for the original loss  $f$  after substituting  $x^{\text{adv}}$  for  $x$  in  $f(x, y; \theta)$ . The final update formula is:

$$\theta \leftarrow \text{Proj}_{\{\theta' : \|\theta'\|_0 \leq k\}}(\theta - \lambda_t \nabla_{\theta} f(x^{\text{adv}}, y; \theta)).$$

**Finding the Worst Adversary** Now the last roadblock is how to find the “worst adversary”  $x^{\text{adv}}$ . This essentially becomes another optimization problem of solving equation 1, while the adversarial input is the target variable rather than the network parameters. We use the sign-SGD algorithm [Bernstein et al., 2018] to cope with this sub-problem. The update formula for the  $i$ -th iteration is as below:

$$x_{i+1}^{\text{adv}} = \text{Proj}_{\{x' : \|x' - x\|_{\infty} \leq \rho\}} \{x_i^{\text{adv}} + \alpha \text{sign}(\nabla_x f(x_i^{\text{adv}}, y; \theta))\}.$$

Here, we use  $\nabla_x f(\cdot; \cdot)$  to obtain the gradient in terms of the image term, and use the sign of this gradient to update the adversary. Then we project the updated adversary back to the feasible region. Our approach follows the idea of the IFGSM attack [Kurakin et al., 2016]. The recent study [Bernstein et al., 2018] validates the convergence of sign (stochastic) gradient descent.

### 3 Experiments

To demonstrate that ATMC achieves the remarkably favorable trade-off between robustness and efficiency, we have carefully designed two main groups of experiments:

---

**Algorithm 1** ATMC

---

**Input:** dataset  $\mathcal{Z}$ , stepsize sequence  $\{\lambda_t > 0\}_{t=0}^{T-1}$ , update steps  $n$  and  $T$ , hyper-parameter  $\rho$  and  $k$   
**Output:** model  $\theta$   
 $\alpha \leftarrow 1.25\rho/n$   
Initialize  $\theta$   
**for**  $t = 0$  to  $T - 1$  **do**  
  Sample  $(x, y)$  from  $\mathcal{Z}$   
   $x^{\text{adv}} \leftarrow x$   
  **for**  $i = 0$  to  $n - 1$  **do**  
     $\Delta = \alpha \text{sign}(\nabla_x f(\theta; x^{\text{adv}}, y))$   
     $x^{\text{adv}} \leftarrow \text{Proj}_{\{x': \|x' - x\|_\infty \leq \rho\}}\{x^{\text{adv}} + \Delta\}$   
  **end for**  
   $\theta \leftarrow \text{Proj}_{\{\theta': \|\theta'\|_0 \leq k\}}(\theta - \lambda_t \nabla_{\theta} f(\theta; x^{\text{adv}}, y))$   
**end for**

---

Table 1: The CNN models used in the experiments.

Models	#Parameters	Dataset & Accuracy
LeNet	430K	MNIST: 99.32%
ResNet	21M	CIFAR-10: 93.67%
ConvNet	1M	STL-10: 77.58%
WideResNet	11M	SVHN: 95.25%

- When compressing state-of-the-art CNNs, how ATMC compares with sequential baselines of mixing or iterating between applying compression and defense methods (Section 3.2).
- How the compressed models by ATMC compare with off-the-shelf light-weight CNNs (e.g. MobileNet) with strong defense methods applied (Section 3.3).

We further address two relevant concerns:

- Whether ATMC is compatible with a post-processing step of quantization (Section 3.4).
- Whether the robustness of compressed models by ATMC can generalize to other (white-box) attackers, given in ATMC algorithm we use IFGSM attack in finding the worst adversary (Section 3.5).

Our evaluation is performed with a variety of popular datasets, benchmark models, and metrics, as summarized next in Section 3.1.

### 3.1 Experimental Setup

**Datasets and Benchmark Models** We select four popular image classification datasets and pick one top-performer CNN model on each dataset: i) LeNet<sup>1</sup> on the MNIST dataset [LeCun et al., 1998]; ii) ResNet [He et al., 2016] on the CIFAR-10 dataset [Krizhevsky and Hinton, 2009]; iii) ConvNet<sup>2</sup> on the STL-10 dataset [Coates et al., 2011]; and iv) WideResNet [Zagoruyko and Komodakis, 2016] on the SVHN dataset [Netzer et al., 2011]. Their details are summarized in Table 1.

---

<sup>1</sup>[github.com/BVLC/caffe/blob/master/examples/mnist](https://github.com/BVLC/caffe/blob/master/examples/mnist)

<sup>2</sup>[github.com/aaron-xichen/pytorch-playground](https://github.com/aaron-xichen/pytorch-playground). We used their pre-trained model on STL10.

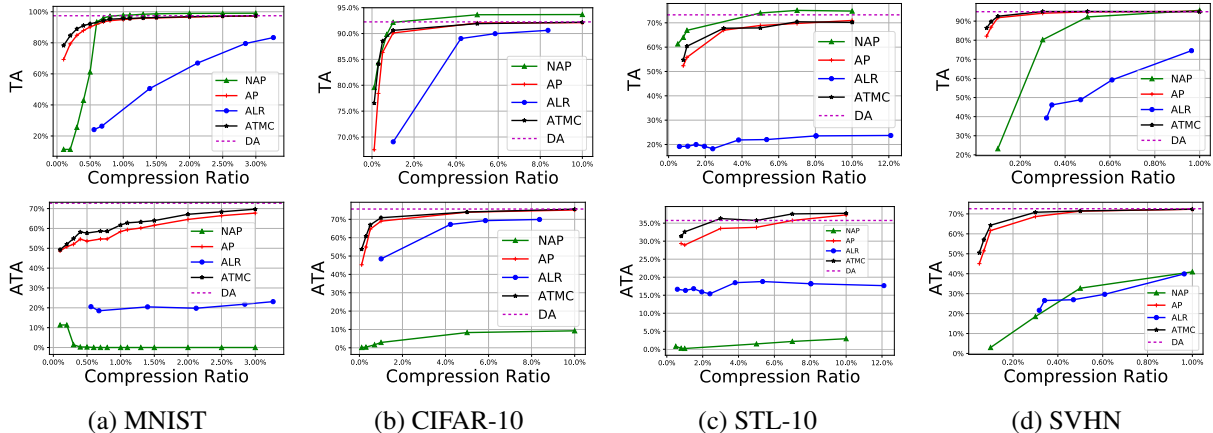


Figure 1: Comparison among NAP, AP, ALR and ATMC on four models/datasets. **Top row:** TA versus compression ratio. **Bottom row:** ATA versus compression ratio. The purple dashed lines mark the the original model results.

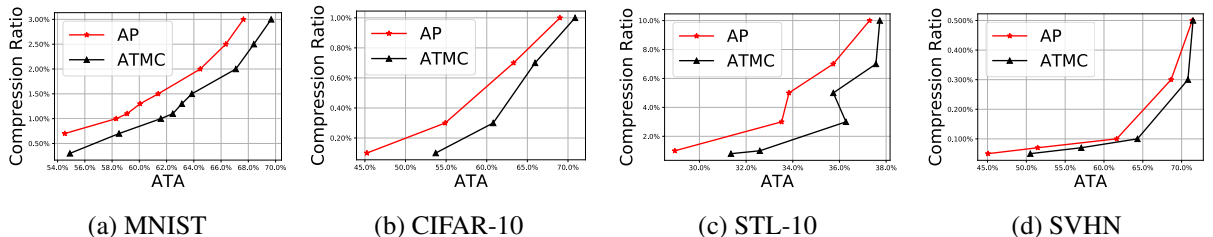


Figure 2: Zoom-in comparison between ATMC and AP against the adversarial samples with various compression ratios.

**Evaluation Metrics** We adopt a variety of different metrics to evaluate the target robustness-efficiency trade-off, from different settings and perspectives.

**Testing Accuracy (TA):** unless otherwise noted, TA denotes the standard top-1 classification accuracy on the original testing set of each dataset.

**Adversarial Testing Accuracy (ATA):** we first apply an attack algorithm to generate an adversarial sample for each sample in the original testing set, creating an *adversarial testing set*. ATA denotes the top-1 classification accuracy on this adversarial testing set, serving as an indicator of model robustness to adversarial attacks.

**Parameter Number:** the number of non-zero parameters.

**Compression Ratio:** the ratio between the parameter number of the compressed model and that of the original model.

**Attack Settings** Unless otherwise stated (e.g., in Section 3.5), we apply the IFGSM attacker [Kurakin et al., 2016] to find adversarial samples for both training and testing. Following the PGD [Madry et al., 2017] adversarial attack setting, we set the perturbation magnitude  $\rho$  for MNIST, CIFAR-10, STL-10, SVHN as 0.3, 0.06, 0.03, and 0.06, respectively and the color scale of each channel is normalized between [0,1].

We train ATMC for 50 epochs on MNIST using P-SGD, and for 150 epochs on CIFAR-10, STL-10, and SVHN. The learning rate  $\lambda_t$  is set as 0.005 for all at the beginning and decreases by 10% at 30<sup>th</sup>, 60<sup>th</sup>,

90<sup>th</sup>, and 120<sup>th</sup> epoch. To find the adversary, we run IFGSM for 16 iterations on MNIST, and 3 on the other three datasets. Each reported ATA is averaged from three IFGSM training results with different random initializations, although we always find them quite close.

### 3.2 Comparison to Pure Compression, Pure Defense, and Their Mixtures

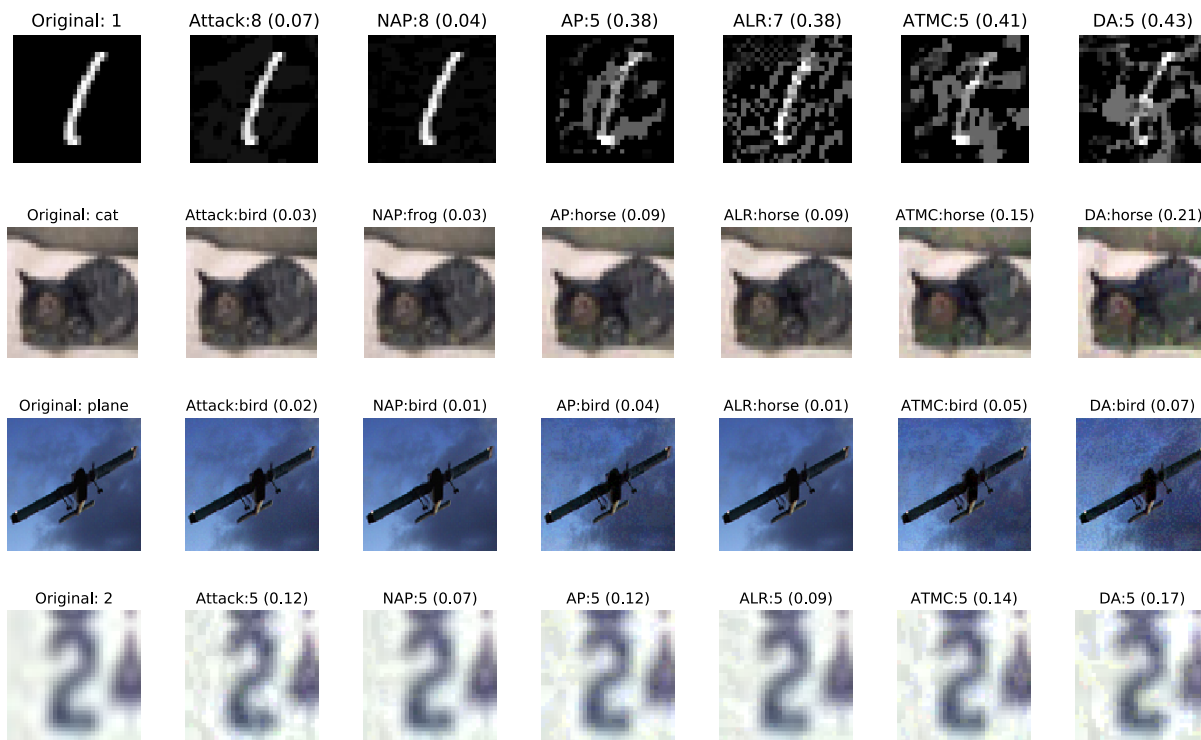


Figure 3: Visualization of the smallest magnitude adversarial perturbations found to fool the original models; and then the models compressed by NAP, AP, ALR, ATMC; and the model defended by applying DA (no compression), respectively. From top to bottom are examples from MNIST (class “1”), CIFAR-10 (class “cat”), STL-10 (class “plane”), and SVNH (class “2”). The attack magnitudes found are in corresponding parentheses.

Since no existing work directly pursues our same goal of simultaneous robustness and efficiency, we start from two straightforward baselines to be compared with ATMC: standard compression (without defense), and standard defense (without compression). Furthermore, we could craft “mixture” baselines to achieve the goal: first applying a defense method on a dense model, then compressing it, and eventually fine-tuning the compressed model (with parameter number unchanged, e.g., by fixing zero elements) using the defense method again. In view of them, we design the following baselines to compare with ATMC:

- *Non-Adversarial Pruning (NAP)*: we train a dense state-of-the-art CNN and then compress it by pruning: only keeping the largest-magnitudes weight elements while setting others to zero. We then fine-tune the nonzero weights (with zero weights fixed) on the training set again until convergence. NAP can thus explicitly control the compressed model size in the same way as ATMC. There is no defense performed in NAP.



- *Dense Adversarial Training (DA)*: we apply adversarial training [Kurakin et al., 2016] to defend a dense CNN, with no compression performed.
- *Adversarial Pruning (AP)*: we first apply the defensive method [Kurakin et al., 2016] to pre-train a defense CNN. We then prune the dense model into a sparse one, and fine-tune the non-zero weights of pruned model until convergence, similarly to NAP.
- *Adversarial Low-Rank Decomposition (ALR)*: it is all similar to the AP routine, except that we use low rank factorization [Tai et al., 2015] in place of pruning to achieve the compression step.

Fig 1 compares the TA (top row) and ATA (bottom row) variations w.r.t. the compression ratios, and reveals a number of important observations. First, while NAP can often obtain decent TA results at compression (e.g., it yields the best original test set accuracies on CIFAR-10 and STL-10), it becomes deteriorated in terms of robustness to adversarial attacks (quantified by ATA). That verifies our motivating intuition: *naive compression can significantly compromise robustness*. The observation also raises a red flag for typical CNN compression evaluation, where the robustness of compressed models is (almost completely) overlooked.

Second, while both AP and ALR jointly consider compression and defense in ad-hoc sequential ways, ATMC further gains notably advantages the two, in achieving superior trade-offs between TA/ATA and compression ratios. That is owing to the unified optimization form of ATMC, as well as the new decomposition structure (3) that allows for more flexible compression. We also provide zoom-in views in Fig 2 to more clearly display the performance margin of ATMC over AP (its closest competitor).

Third, ATMC achieves comparable accuracy (TA) and robustness (ATA) to DA, with minimal amounts of parameters after compression. Meanwhile, ATMC also achieves very close, sometimes better TA-compression ratio trade-offs than NAP, with much enhanced robustness (ATA). Therefore, it has indeed combined the best of both worlds. It is also noteworthy that those ATMC-compressed models possess very close TAs and ATAs, compared to the much larger original models (uncompressed/undefended; marked by dashed lines in each figure),

Fig 3 further visualizes the robustness of different methods to adversarial attacks. On each dataset, we gradually increase the the IFGSM attack magnitude to find the “smallest-magnitude adversarial perturbation” needed to fool each model (original model; compressed models by NAP, AP, ALR, and ATMC into a same parameter number level; and the dense model by DA). Those original models are trained with original training samples for each dataset. Apparently, a more robust model needs a larger-magnitude attack to be confused. Not surprisingly, DA slightly outperforms ATMC, and they both surpass AP and ALR with notable margins. NAP attains the worst robustness and can be confused by tiny perturbations (although its TA still remains to be high).

### 3.3 Comparison to Light-Weight CNNs with Defense

The goal of ATMC is to obtain models which can run efficiently on resource-limited devices and also with robustness adversarial attacks. We notice that an alternative to achieve this goal could be to apply defense methods to those specially-designed light-weight CNN backbones (rather than compressing from large CNNs). Those solutions are compared with ATMC on the CIFAR-10 dataset.

Several representative compact and efficient CNN models are picked: MobileNetV1 [Howard et al., 2017], MobileNetV2 [Sandler et al., 2018], ShuffleNetV1 [Zhang et al., 2017], and ShuffleNetV2 [Ma et al., 2018]. Following their original settings, we vary the channel scale factors for all these four architectures in order to get more models with different complexities. We then apply one of the strongest defense method

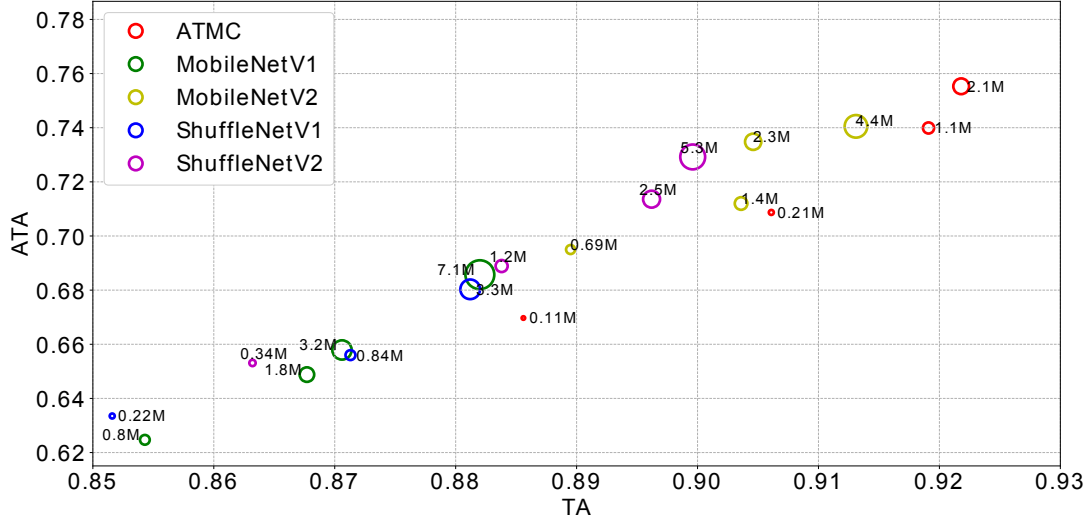


Figure 4: Comparison between ATMC and light-weight CNN solutions, on the TA-ATA trade-off plot. Each marker represents a model, whose size is in proportion to the model’s parameter number.

PGD [Madry et al., 2017] to enhance their robustness. Details on channel scale factor and learning rates can be found in Appendix A.1 and A.2.

We use the same ATMC models trained in Section 3.2 for comparison. Since the compression ratio is no longer applicable here, we plot the trade-off between TA and ATA in Fig 4. Each marker denotes one model: the marker size is proportional to the parameter number, which we also mark aside the marker. As we can see, ATMC can achieve higher TAs and ATAs (i.e., its markers being closer to the top-right of the plot), with much fewer parameters compared with all four efficient CNN options. For instance, ATMC achieves 91.91% TA and 73.99% ATA with around 1.1 million non-zero parameters, while MobileNetV2 achieves similar results with about 4.4 million non-zero parameters. As another example, with as few as 107k parameters, the TA/ATA performance of ATMC is still more favorable than MobileNetV1 with 3.2 million parameters and ShuffleNetV1 with 840k parameters. More detailed experimental results can be found in Appendix A.2 and B.1.

Table 2 manifests that original efficient CNNs have high TAs, but not naturally high ATAs. Applying adversarial training as a defensive method on them hurts their TAs. By contrast, ATMC benefits from the simultaneous optimization on efficiency and robustness, achieving better robustness with smaller models.

### 3.4 Compatibility with Quantization Post-Processing

When deploying deep models onto resource-limited devices, neural network weights are usually quantized from 32-bit floating point numbers to lower precision, such as 16-bits or 8-bits. Will the performance advantage of ATMC persist after quantization?

We choose the compressed models by ATMC, ALR, AP and NAP on CIFAR-10 that are used in Section 3.2, and further apply standard linear scalar quantization [Vanhoucke et al., 2011] to quantize all their weight elements to 8 bits. As shown in Fig 5, the results suggest that NAP and AP appear to be quite fragile to parameter quantization, and both witness significant TA and ATA drops. In contrast, ATMC and ALR seem

Table 2: The models with best TAs, as well as their sizes and ATAs, from the four efficient CNNs (without/with defense) as well as the ATMC-compressed models, on the CIFAR-10 dataset. Best results among defensive methods and the best TA among all methods are shown in **bold** text. The configurations of those best models could be referred to the supplementary.

Models	#Parameters	TA	ATA
MobileNetV1 (original)	7.1M	92.58%	7.9%
MobileNetV1 (defended)	7.1M	88.2%	68.57%
MobileNetV2 (original)	4.4M	<b>94.24%</b>	3.51%
MobileNetV2 (defended)	4.4M	91.31%	74.05%
ShuffleNetV1 (original)	3.3M	92.55%	10.36%
ShuffleNetV1 (defended)	3.3M	88.12%	68.03%
ShuffleNetV2 (original)	5.3M	93.39%	7.44%
ShuffleNetV2 (defended)	5.3M	89.96%	72.92%
ATMC	<b>2.1M</b>	<b>92.18%</b>	<b>75.53%</b>

to be almost unaffected by quantization: in both plots, their new dash-lines nearly overlap with original solid lines. Therefore, ATMC is readily amendable to the post-processing of quantization if smaller model sizes are desired. We further plan to integrate quantization into the ATMC structural constraint (3) in future work.

### 3.5 Generalized Robustness Against Other Attackers

In all previous experiments, we have only tested ATMC and the baseline methods against one attack algorithm IFGSM [Kurakin et al., 2016]. We will now show that ATMC also outperforms the baseline methods when facing other attacking methods. Specifically, we show the results against FGSM [Goodfellow et al., 2014] and WRM [Sinha et al., 2017] in Fig 6. We select these two methods because they are complementary to IFGSM: IFGSM is an iterative  $\ell_\infty$  attacker, while FGSM is a one-step  $\ell_\infty$  attacker and WRM is an iterative  $\ell_2$  attacker. We set the adversarial iteration step to be 7 in WRM and  $\epsilon$  to be 0.06 in FGSM. As we can see, ATMC outperforms its strongest competitor AP in all cases except one where they get very close accuracy against FGSM at the compression ratio of 5%.

## 4 Conclusion

This paper aims to address the new problem of simultaneously achieving high robustness and compactness in CNN models. We propose the ATMC framework, by integrating the two goals in one unified constrained optimization framework. Our extensive experiments endorse the effectiveness of ATMC by observing the following: i) naive model compression may hurt robustness, if the latter is not explicitly taken into account; ii) a proper joint optimization could let robustness and efficiency benefit from each other; in that way, a compressed model could even maintain almost the same accuracy and robustness compared to the original one; iii) the compressed models can remain robust under further quantization and against different attackers.

## References

- A. Athalye and I. Sutskever. Synthesizing robust adversarial examples. *arXiv preprint arXiv:1707.07397*, 2017.
- A. Athalye, N. Carlini, and D. Wagner. Obfuscated gradients give a false sense of security: Circumventing defenses to adversarial examples. *arXiv preprint arXiv:1802.00420*, 2018.
- J. Bernstein, Y.-X. Wang, K. Azizzadenesheli, and A. Anandkumar. signsgd: compressed optimisation for non-convex problems. *arXiv preprint arXiv:1802.04434*, 2018.
- E. J. Candès, X. Li, Y. Ma, and J. Wright. Robust principal component analysis? *Journal of the ACM (JACM)*, 58(3):11, 2011.
- N. Carlini and D. Wagner. Towards evaluating the robustness of neural networks. In *2017 IEEE Symposium on Security and Privacy (SP)*, pages 39–57. IEEE, 2017.
- Y. Cheng, D. Wang, P. Zhou, and T. Zhang. A survey of model compression and acceleration for deep neural networks. *arXiv preprint arXiv:1710.09282*, 2017.
- A. Coates, A. Ng, and H. Lee. An analysis of single-layer networks in unsupervised feature learning. In *Proceedings of the fourteenth international conference on artificial intelligence and statistics*, pages 215–223, 2011.
- M. Courbariaux, Y. Bengio, and J.-P. David. Binaryconnect: Training deep neural networks with binary weights during propagations. In *Advances in neural information processing systems*, pages 3123–3131, 2015.
- J. M. Danskin. *The theory of max-min and its application to weapons allocation problems*, volume 5. Springer Science & Business Media, 2012.
- J. Deng, W. Dong, R. Socher, L.-J. Li, K. Li, and L. Fei-Fei. ImageNet: A Large-Scale Hierarchical Image Database. In *CVPR09*, 2009.
- E. L. Denton, W. Zaremba, J. Bruna, Y. LeCun, and R. Fergus. Exploiting linear structure within convolutional networks for efficient evaluation. In *Advances in neural information processing systems*, pages 1269–1277, 2014.
- G. S. Dhillon, K. Azizzadenesheli, J. D. Bernstein, J. Kossaifi, A. Khanna, Z. C. Lipton, and A. Anandkumar. Stochastic activation pruning for robust adversarial defense. In *International Conference on Learning Representations*, 2018.
- Y. Gong, L. Liu, M. Yang, and L. Bourdev. Compressing deep convolutional networks using vector quantization. *arXiv preprint arXiv:1412.6115*, 2014.
- I. J. Goodfellow, J. Shlens, and C. Szegedy. Explaining and harnessing adversarial examples. *CoRR*, abs/1412.6572, 2014.
- Y. Guo, C. Zhang, C. Zhang, and Y. Chen. Sparse dnns with improved adversarial robustness. *arXiv preprint arXiv:1810.09619*, 2018.

- S. Han, H. Mao, and W. J. Dally. Deep compression: Compressing deep neural networks with pruning, trained quantization and huffman coding. *arXiv preprint arXiv:1510.00149*, 2015a.
- S. Han, J. Pool, J. Tran, and W. Dally. Learning both weights and connections for efficient neural network. In *Advances in neural information processing systems*, pages 1135–1143, 2015b.
- K. He, X. Zhang, S. Ren, and J. Sun. Deep residual learning for image recognition. In *Proceedings of the IEEE conference on computer vision and pattern recognition*, pages 770–778, 2016.
- J. Hendrik Metzen, M. Chaithanya Kumar, T. Brox, and V. Fischer. Universal adversarial perturbations against semantic image segmentation. In *Proceedings of the IEEE Conference on Computer Vision and Pattern Recognition*, pages 2755–2764, 2017.
- H. Hosseini, Y. Chen, S. Kannan, B. Zhang, and R. Poovendran. Blocking transferability of adversarial examples in black-box learning systems. *arXiv preprint arXiv:1703.04318*, 2017.
- A. G. Howard, M. Zhu, B. Chen, D. Kalenichenko, W. Wang, T. Weyand, M. Andreetto, and H. Adam. Mobilenets: Efficient convolutional neural networks for mobile vision applications, 2017.
- J. Jin, A. Dundar, and E. Culurciello. Flattened convolutional neural networks for feedforward acceleration. *arXiv preprint arXiv:1412.5474*, 2014.
- A. Krizhevsky and G. Hinton. Learning multiple layers of features from tiny images. Technical report, Citeseer, 2009.
- A. Kurakin, I. J. Goodfellow, and S. Bengio. Adversarial machine learning at scale. *CoRR*, abs/1611.01236, 2016.
- V. Lebedev, Y. Ganin, M. Rakhuba, I. Oseledets, and V. Lempitsky. Speeding-up convolutional neural networks using fine-tuned cp-decomposition. *arXiv preprint arXiv:1412.6553*, 2014.
- Y. LeCun, L. Bottou, Y. Bengio, and P. Haffner. Gradient-based learning applied to document recognition. *Proceedings of the IEEE*, 86(11):2278–2324, 1998.
- H. Li, A. Kadav, I. Durdanovic, H. Samet, and H. P. Graf. Pruning filters for efficient convnets. *arXiv preprint arXiv:1608.08710*, 2016.
- F. Liao, M. Liang, Y. Dong, T. Pang, X. Hu, and J. Zhu. Defense against adversarial attacks using high-level representation guided denoiser. In *Proceedings of the IEEE Conference on Computer Vision and Pattern Recognition*, pages 1778–1787, 2018.
- B. Liu, M. Wang, H. Foroosh, M. Tappen, and M. Pensky. Sparse convolutional neural networks. In *Proceedings of the IEEE Conference on Computer Vision and Pattern Recognition*, pages 806–814, 2015.
- B. Luo, Y. Liu, L. Wei, and Q. Xu. Towards imperceptible and robust adversarial example attacks against neural networks. *arXiv preprint arXiv:1801.04693*, 2018.
- N. Ma, X. Zhang, H.-T. Zheng, and J. Sun. Shufflenet v2: Practical guidelines for efficient cnn architecture design. In *Proceedings of the European Conference on Computer Vision (ECCV)*, pages 116–131, 2018.
- A. Madry, A. Makelov, L. Schmidt, D. Tsipras, and A. Vladu. Towards deep learning models resistant to adversarial attacks. *arXiv preprint arXiv:1706.06083*, 2017.

- D. Meng and H. Chen. Magnet: a two-pronged defense against adversarial examples. In *Proceedings of the 2017 ACM SIGSAC Conference on Computer and Communications Security*, pages 135–147. ACM, 2017.
- S.-M. Moosavi-Dezfooli, A. Fawzi, and P. Frossard. Deepfool: a simple and accurate method to fool deep neural networks. In *Proceedings of the IEEE Conference on Computer Vision and Pattern Recognition*, pages 2574–2582, 2016.
- P. Nakkiran, R. Alvarez, R. Prabhavalkar, and C. Parada. Compressing deep neural networks using a rank-constrained topology. In *Sixteenth Annual Conference of the International Speech Communication Association*, 2015.
- Y. Netzer, T. Wang, A. Coates, A. Bissacco, B. Wu, and A. Y. Ng. Reading digits in natural images with unsupervised feature learning. In *NIPS workshop on deep learning and unsupervised feature learning*, volume 2011, page 5, 2011.
- B. Neyshabur and R. Panigrahy. Sparse matrix factorization. *arXiv preprint arXiv:1311.3315*, 2013.
- N. Papernot and P. McDaniel. Extending defensive distillation. *arXiv preprint arXiv:1705.05264*, 2017.
- N. Papernot, P. McDaniel, X. Wu, S. Jha, and A. Swami. Distillation as a defense to adversarial perturbations against deep neural networks. In *2016 IEEE Symposium on Security and Privacy (SP)*, pages 582–597. IEEE, 2016.
- M. Rastegari, V. Ordonez, J. Redmon, and A. Farhadi. Xnor-net: Imagenet classification using binary convolutional neural networks. In *European Conference on Computer Vision*, pages 525–542. Springer, 2016.
- M. Sandler, A. Howard, M. Zhu, A. Zhmoginov, and L.-C. Chen. Mobilenetv2: Inverted residuals and linear bottlenecks. In *2018 IEEE/CVF Conference on Computer Vision and Pattern Recognition*, pages 4510–4520. IEEE, 2018.
- A. Sinha, H. Namkoong, and J. Duchi. Certifiable distributional robustness with principled adversarial training. *arXiv preprint arXiv:1710.10571*, 2017.
- C. Tai, T. Xiao, Y. Zhang, X. Wang, et al. Convolutional neural networks with low-rank regularization. *arXiv preprint arXiv:1511.06067*, 2015.
- F. Tramér, A. Kurakin, N. Papernot, D. Boneh, and P. D. McDaniel. Ensemble adversarial training: Attacks and defenses. *arXiv preprint arXiv:1705.07204*, 2017.
- V. Vanhoucke, A. Senior, and M. Z. Mao. Improving the speed of neural networks on cpus. In *Deep Learning and Unsupervised Feature Learning Workshop, NIPS 2011*, 2011.
- W. Wen, C. Wu, Y. Wang, Y. Chen, and H. Li. Learning structured sparsity in deep neural networks. In *Advances in Neural Information Processing Systems*, pages 2074–2082, 2016.
- J. Wu, C. Leng, Y. Wang, Q. Hu, and J. Cheng. Quantized convolutional neural networks for mobile devices. In *Proceedings of the IEEE Conference on Computer Vision and Pattern Recognition*, pages 4820–4828, 2016.

- J. Wu, Y. Wang, Z. Wu, Z. Wang, A. Veeraraghavan, and Y. Lin. Deep k-means: Re-training and parameter sharing with harder cluster assignments for compressing deep convolutions. In *International Conference on Machine Learning*, pages 5359–5368, 2018.
- C. Xie, J. Wang, Z. Zhang, Y. Zhou, L. Xie, and A. Yuille. Adversarial examples for semantic segmentation and object detection. In *International Conference on Computer Vision*. IEEE, 2017.
- W. Xu, D. Evans, and Y. Qi. Feature squeezing: Detecting adversarial examples in deep neural networks. *arXiv preprint arXiv:1704.01155*, 2017.
- X. Yu, T. Liu, X. Wang, and D. Tao. On compressing deep models by low rank and sparse decomposition. In *Proceedings of the IEEE Conference on Computer Vision and Pattern Recognition*, pages 7370–7379, 2017.
- S. Zagoruyko and N. Komodakis. Wide residual networks. *arXiv preprint arXiv:1605.07146*, 2016.
- X. Zhang, X. Zhou, M. Lin, and J. Sun. Shufflenet: An extremely efficient convolutional neural network for mobile devices, 2017.
- H. Zhou, J. M. Alvarez, and F. Porikli. Less is more: Towards compact cnns. In *European Conference on Computer Vision*, pages 662–677. Springer, 2016.
- D. Zügner, A. Akbarnejad, and S. Günnemann. Adversarial attacks on neural networks for graph data. In *Proceedings of the 24th ACM SIGKDD International Conference on Knowledge Discovery & Data Mining*, pages 2847–2856. ACM, 2018.

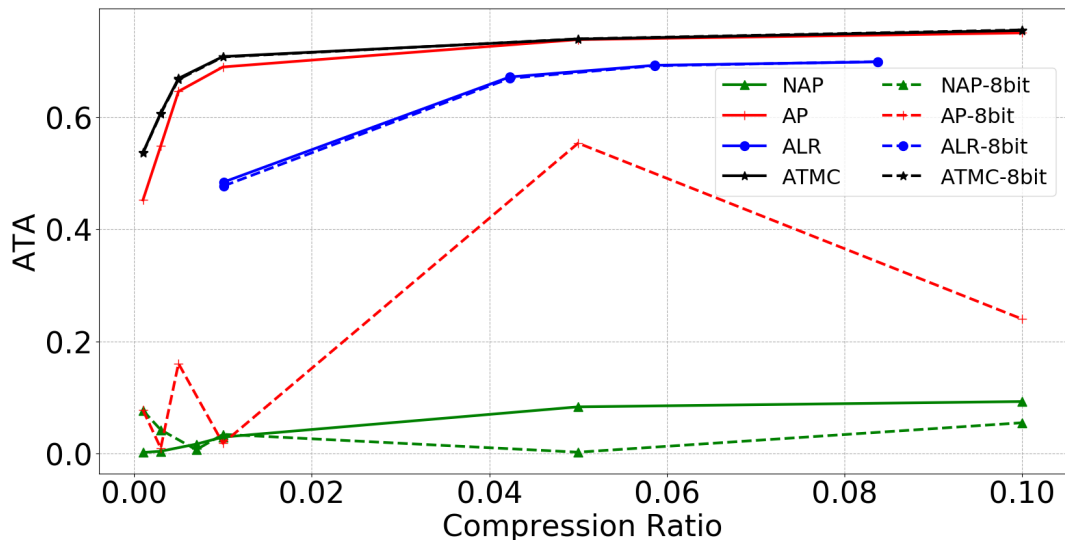
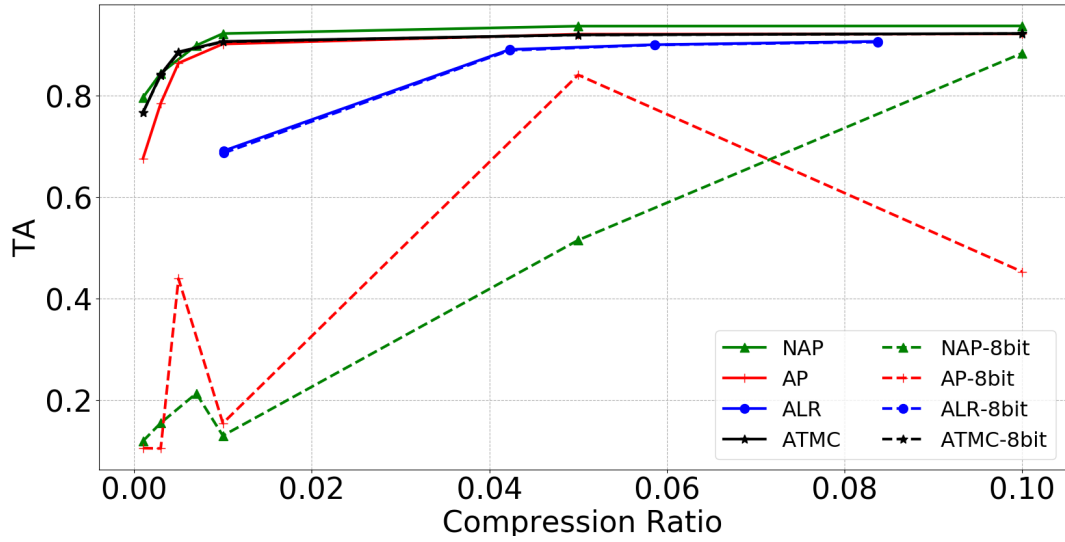


Figure 5: The effect of 8-bit quantization as post-processing, on TA/ATA of various compressed models on CIFAR-10. Solid lines denote the results of (full-precision) compressed models, and the dotted lines are 8-bit model results.



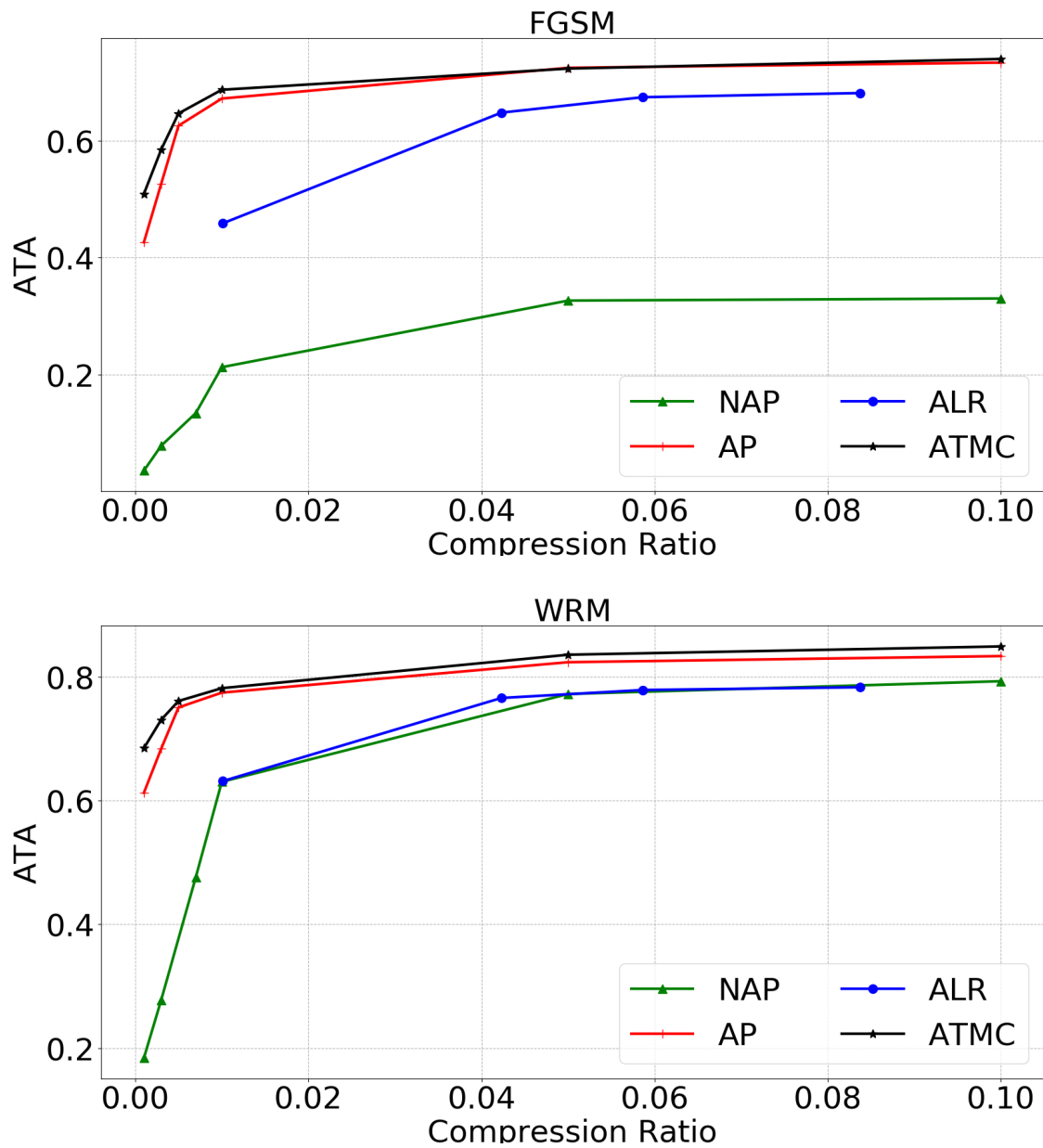


Figure 6: Adversarial testing accuracy against FGSM (top) and WRM (bottom) on CIFAR-10.

## A Comparison between ATMC and Light-Weight CNNs with Defense

### A.1 Light-Weighted CNNs Learning Rate Selection

We tested four different learning rate plans, as shown in Fig 7, on four randomly selected networks (MobileNetV1 1 $\times$ , MobileNetV1 0.5 $\times$ , ShuffleNetV2 1 $\times$  and ShuffleNetV2 2 $\times$ ). We find that, on all these selected networks, plan 1 gets the highest TA for non-adversarial training; plan 1 and plan 3 get similar TA and ATA for adversarial training, outperforming plan 2 and plan 4. Hence, in section 3.3, we apply plan 1 for all non-adversarial training experiments, whose results are shown in Table 2. As for adversarial training experiments, since plan 1 and 3 gets similar results, we randomly choose to apply plan 1 on MobileNetV2 and ShuffleNetV2 and plan 3 on MobileNetV1 and ShuffleNetV1.

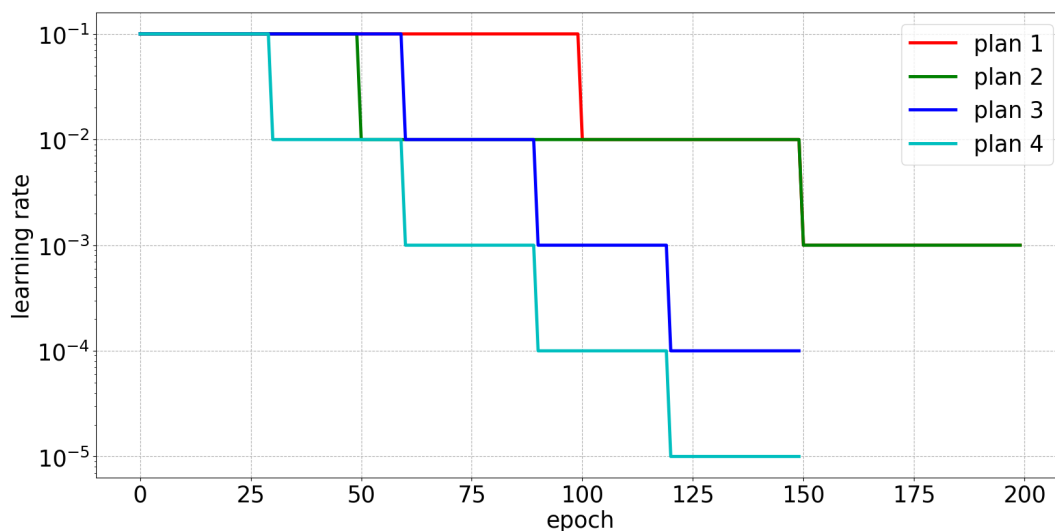


Figure 7: Learning Rate Plans. Plan 1 and plan 2 iterate 200 epochs. Plan 3 and plan 4 iterate 150 epochs.

### A.2 Detailed Experimental Results on Adversarially Trained Light-Weighted Deep Neural Networks

The experimental results on adversarially trained light-weighted deep neural networks are shown in Fig 4. We provide the accuracy values on these experiments in Table 3, 4, 5, and 6. The first row of each Table indicates the hyper-parameter for each model, e.g., MobileNetV1 with scale factor 1.5. The second row shows the corresponding parameter number for a specific light-weighted deep neural network. The third and fourth row shows TA and ATA respectively.

The best models of each efficient network structure in Table 2 are MobileNetV1(1.5 $\times$ ), MobileNetV2(1.4 $\times$ ), ShuffleNetV1( $g=3$ , 2 $\times$ ) and ShuffleNetV2(2 $\times$ ) respectively, as they achieve the highest TA among different configurations of the same network structure.

Table 3: Parameter number, TA and ATA against IFGSM of MobileNetV1.

SCALE FACTOR	1.5	1	0.75	0.5	0.25	0.125
PARAMETER NUMBER	7,147,680	3,195,328	1,807,824	812,768	210,160	56,024
TA	0.882	0.8706	0.8677	0.8543	0.7984	0.7223
ATA AGAINST IFGSM	0.6857	0.6579	0.6488	0.6247	0.5785	0.5047

Table 4: Parameter number, TA and ATA against IFGSM of MobileNetV2.

SCALE FACTOR	1.4	1	0.75	0.5
PARAMETER NUMBER	4,376,489	2,262,280	1,367,222	693,956
TA	0.9131	0.9046	0.9036	0.8895
ATA AGAINST IFGSM	0.7405	0.7348	0.712	0.695

Table 5: Parameter number, TA and ATA against IFGSM of ShuffleNetV1.

GROUP NUMBER/SCALE FACTOR	3/2	3/1.5	3/1	3/0.5
PARAMETER NUMBER	3,300,522	839,022	216,672	57,597
TA	0.8812	0.8713	0.8516	0.8085
ATA AGAINST IFGSM	0.6803	0.656	0.6335	0.5859

Table 6: Parameter number, TA and ATA against IFGSM of ShuffleNetV2.

SCALE FACTOR	2	1.5	1	0.5
PARAMETER NUMBER	5,304,600	2,465,424	1,247,664	344,080
TA	0.8996	0.8962	0.8838	0.8632
ATA AGAINST IFGSM	0.7292	0.7136	0.6889	0.6531

## B Comparison between ATMC and Pure Compression, Pure Defense, Post-processing Quantization and Their Mixtures

In section 3.2, we discuss the experimental studies on ATMC and other adversarially trained model compression strategies. In these experiments, we vary the left parameter number for all these model compression strategies for the comparison based on TA and ATA. Then, we also show that ATMC is robust under the quantization post-process in section 3.4. At last, we put more types of adversarial attackers to test the robustness of ATMC, NAP, AP, and ALR in section 3.5. In addition, we append some detailed experimental results and case studies in this section to support the learning capability of our ATMC method.

Table 7: Results of ATMC trained ResNet model and post-quantized one against IFGSM, FGSM, and WRM attacks on CIFAR-10 dataset.

<b>compression ratio</b>	0.0010	0.0030	0.0050	0.0100	0.0500	0.1000
<b>parameter number</b>	22,161	64,691	107,221	213,547	1,064,150	2,127,405
<b>TA</b>	0.7655	0.8415	0.8856	0.9061	0.9191	0.9218
<b>ATA against IFGSM</b>	0.5372	0.6079	0.6697	0.7087	0.7399	0.7553
<b>ATA against FGSM</b>	0.5089	0.5847	0.6463	0.6867	0.7229	0.7393
<b>ATA against WRM</b>	0.6847	0.7306	0.7609	0.7816	0.8357	0.8491
<b>TA after 8-bit quantization</b>	0.7665	0.8393	0.8839	0.9054	0.9188	0.9215
<b>ATA against IFGSM after 8-bit quantization</b>	0.5361	0.6064	0.6678	0.7079	0.7403	0.7563

Table 8: Results of ALR trained ResNet model and post-quantized one against IFGSM, FGSM, and WRM attacks on CIFAR-10 dataset.

<b>compression ratio</b>	0.0101	0.0423	0.0586	0.0837
<b>parameter number</b>	214,561	899,287	1,245,143	1,780,082
<b>TA</b>	0.6907	0.8903	0.8997	0.9062
<b>ATA against IFGSM</b>	0.4846	0.6723	0.6931	0.6992
<b>ATA against FGSM</b>	0.4586	0.6477	0.674	0.6811
<b>ATA against WRM</b>	0.6314	0.7658	0.7787	0.7831
<b>TA after 8-bit quantization</b>	0.6863	0.8885	0.8992	0.9049
<b>ATA against IFGSM after 8-bit quantization</b>	0.4777	0.6698	0.6922	0.6997

Table 9: Results of AP trained ResNet model and post-quantized one against IFGSM, FGSM, and WRM attacks on CIFAR-10 dataset

<b>compression ratio</b>	0.0010	0.0030	0.0050	0.0100	0.0500	0.1000
<b>parameter number</b>	22,161	64,691	107,221	213,547	1,064,150	2,127,405
<b>TA</b>	0.6754	0.7842	0.8634	0.9011	0.9204	0.921
<b>ATA against IFGSM</b>	0.4525	0.5489	0.6465	0.6901	0.739	0.751
<b>ATA against FGSM</b>	0.4263	0.5262	0.6254	0.6717	0.7242	0.7331
<b>ATA against WRM</b>	0.6125	0.6839	0.7505	0.7744	0.8236	0.8335
<b>TA after 8-bit quantization</b>	0.1048	0.1042	0.4388	0.154	0.8401	0.4523
<b>ATA against IFGSM after 8-bit quantization</b>	0.0772	0.0093	0.1603	0.0178	0.554	0.2398

## B.1 Experimental Results on ATMC, ALR, AP and NAP

The results of ResNet on CIFAR-10 dataset used in Fig 1, 5, and 6 are provided in Table 7, 8, 9, and 10. The first row indicates the ratio of non-zero parameters left with model compression. And the second row shows the non-zero parameters in total for each model. After the TA score, each row represents the ATA scores under different experimental settings.

Table 10: Results of NAP trained ResNet model and post-quantized one against IFGSM, FGSM, and WRM attacks on CIFAR-10 dataset.

<b>compression ratio</b>	0.0010	0.0030	0.0070	0.0100	0.0500	0.1000
<b>parameter number</b>	22,161	64,691	149,752	213,547	1,064,150	2,127,405
<b>TA</b>	0.7956	0.8435	0.8982	0.9216	0.9363	0.9367
<b>ATA against IFGSM</b>	0.0015	0.0037	0.0164	0.029	0.083	0.0925
<b>ATA against FGSM</b>	0.0365	0.079	0.1348	0.2131	0.3268	0.3304
<b>ATA against WRM</b>	0.1838	0.2777	0.4764	0.6303	0.7722	0.7929
<b>TA after 8-bit quantization</b>	0.1188	0.1544	0.2126	0.1294	0.5146	0.883
<b>ATA against IFGSM after 8-bit quantization</b>	0.0764	0.042	0.0063	0.0339	0.002	0.0546

## B.2 Case study: Ranks of Layers in Adversarially Compressed DNNs

With respect to equation 3, we are acknowledged that ATMC could train the DNNs into a partially low-rank representation  $UV$  for the weights of each layer automatically, where  $U \in \mathbb{R}^{m \times r}$ ,  $V \in \mathbb{R}^{r \times n}$ , and  $r$  is the rank of the corresponding matrix. Hence, we propose a case study that given an specific parameter number, how ATMC can learn the sparse model to be and how low-rank the model can become. For four benchmark DNNs for MNIST, CIFAR-10, STL-10, and SVHN, we choose 1,292, 22,161, 9,022, and 10,954 respectively as the ones to be illustrated in Fig 8, 10, 9, and 11. We treat the number of non-zero

Table 11: Parameter Number for Fig 8, 10, 9, and 11

<b>Dataset</b>	MNIST	CIFAR-10	STL-10	SVHN
<b>DNN Model</b>	LeNet	ResNet	ConvNet	WideResNet
<b># Parameter</b>	1,292	22,161	9,022	10,954

columns of  $U$  as  $r$  for  $U$  and the number of non-zero rows of  $V$  as  $r$  for  $V$ . We record  $r$  for both  $U$  and  $V$  for each layer of different DNNs. Then we draw two bars representing  $r$  for  $U$  and  $V$  together for each layer. As shown in these figures, we can observe that some layers of DNNs are clearly with small  $r$  of either  $U$  or  $V$  which indicates that ATMC do direct the model sparsification to a low-rank structure.

## B.3 More visualization of the smallest magnitude adversarial perturbations found to fool various models

To visualize the defense performance of different methods against adversarial attacks, we gradually increase the IFGSM attack magnitue to find the “smallest-magnitude adversarial pertubation” needed to fool each model (original model; compressed models by NAP, AP, ALR, and ATMC; and the dense model via DA) for all four datasets. All compressed models are restricted to the same parameter number level for a corresponding dataset. Since models obtained via ALR are restricted with low-rank constraints, we choose the closest parameter number of models via ALR to other three strategies. For LeNet on MNIST, we choose the parameter number as 4,305. For ResNet on CIFAR-10, we choose the parameter number as 213,547. For ConvNet on STL-10, we choose the parameter number as 33,833. For WideResNet on SVHN, we choose the

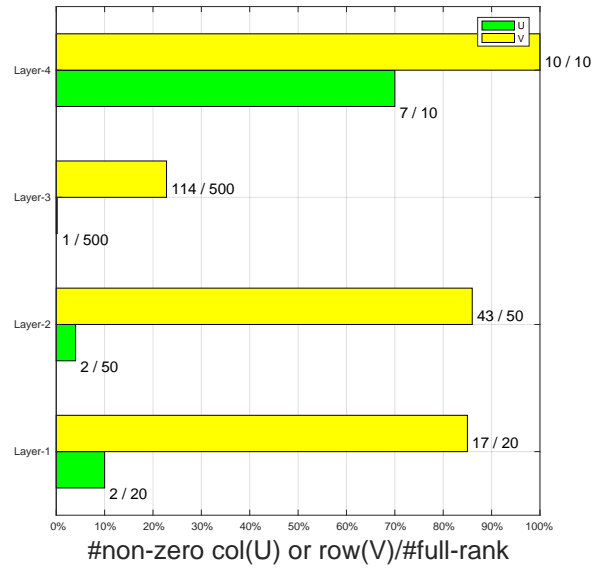


Figure 8: ATMC trained LeNet: Rank  $r$  for  $U$  and  $V$  of each layer.

parameter number as 32,862. At last, we provide the attack cases in Fig 12, 13, 14, and 15.

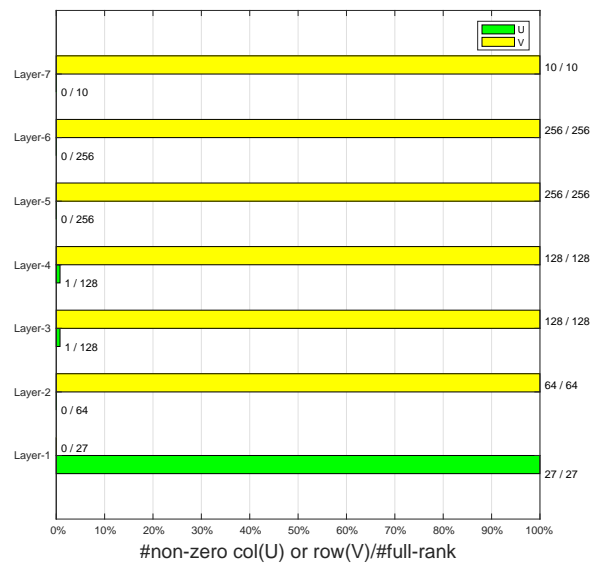


Figure 9: ATMC trained ConvNet: Rank  $r$  for  $U$  and  $V$  of each layer.

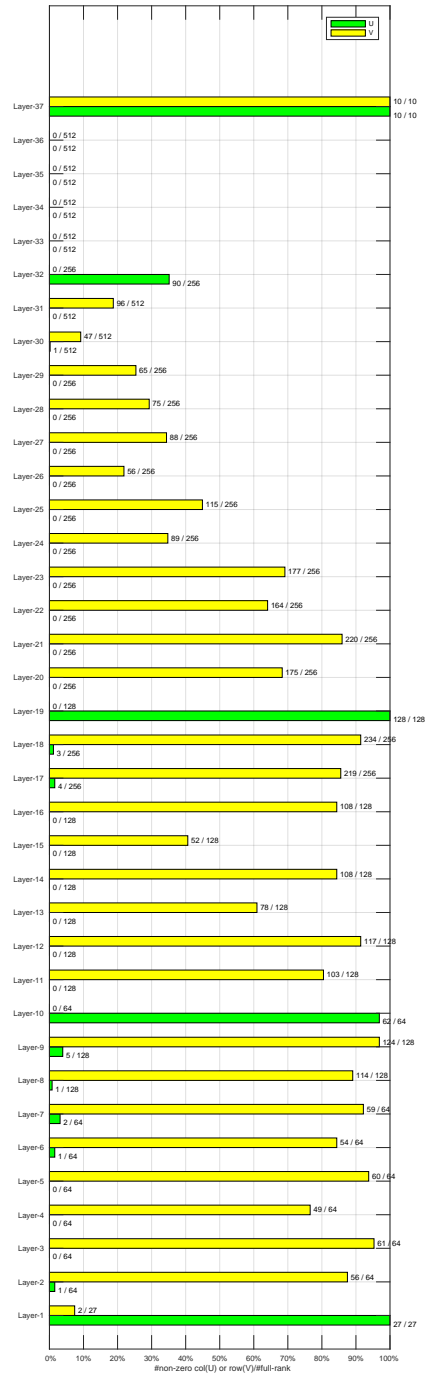


Figure 10: ATMC trained ResNet: Rank  $r$  for  $U$  and  $V$  of each layer.



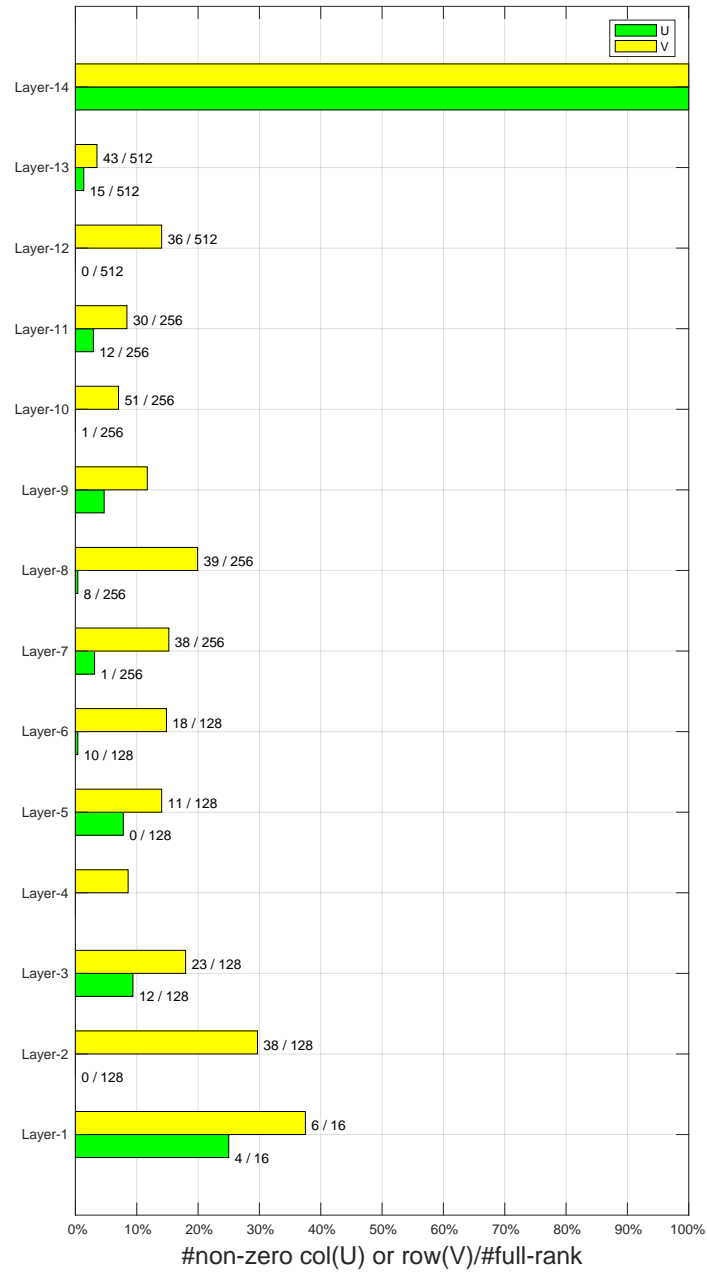


Figure 11: ATMC trained WideResNet: Rank  $r$  for  $U$  and  $V$  of each layer.

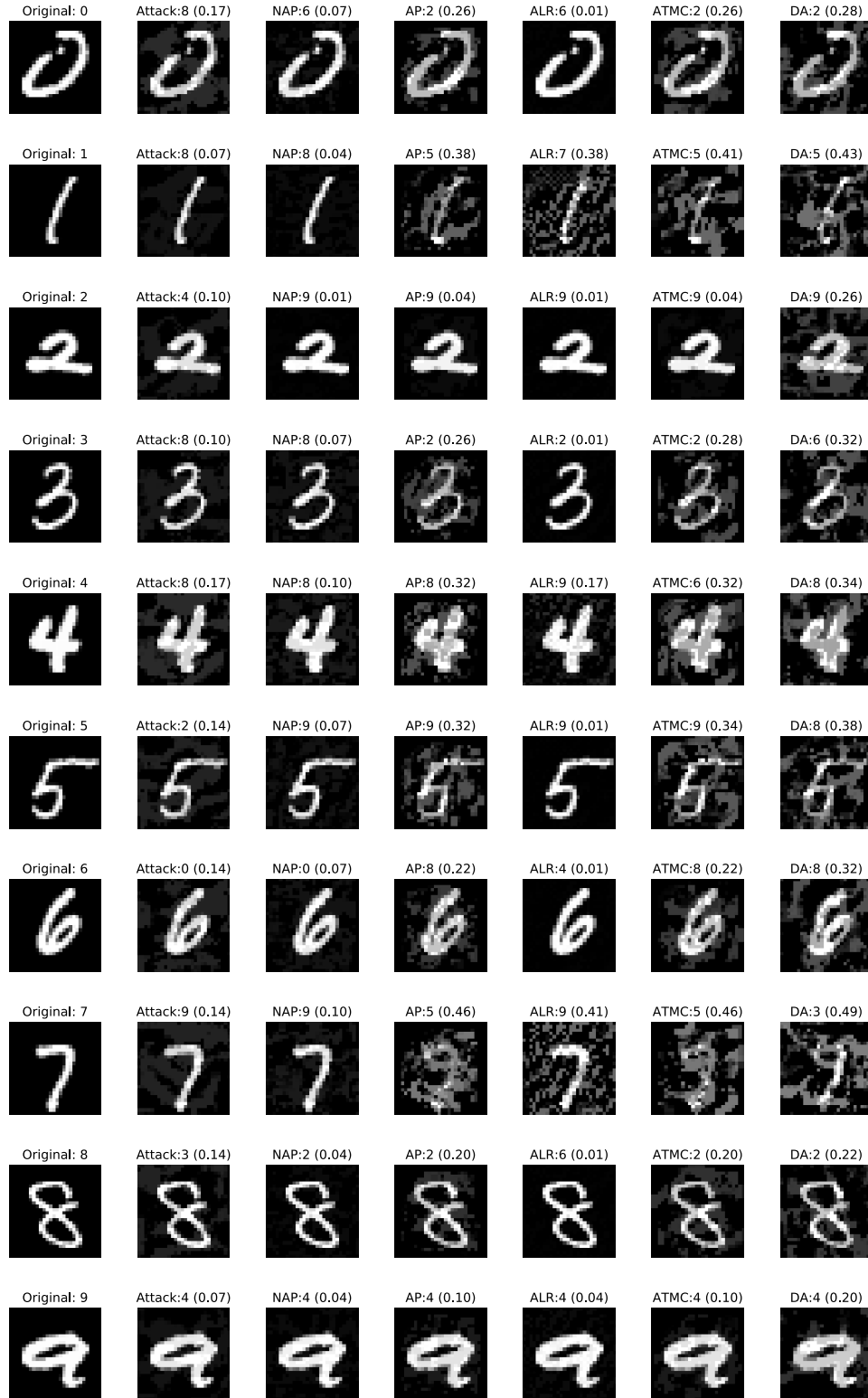


Figure 12: Visualization of the smallest magnitude adversarial perturbations found to fool models on MNIST dataset

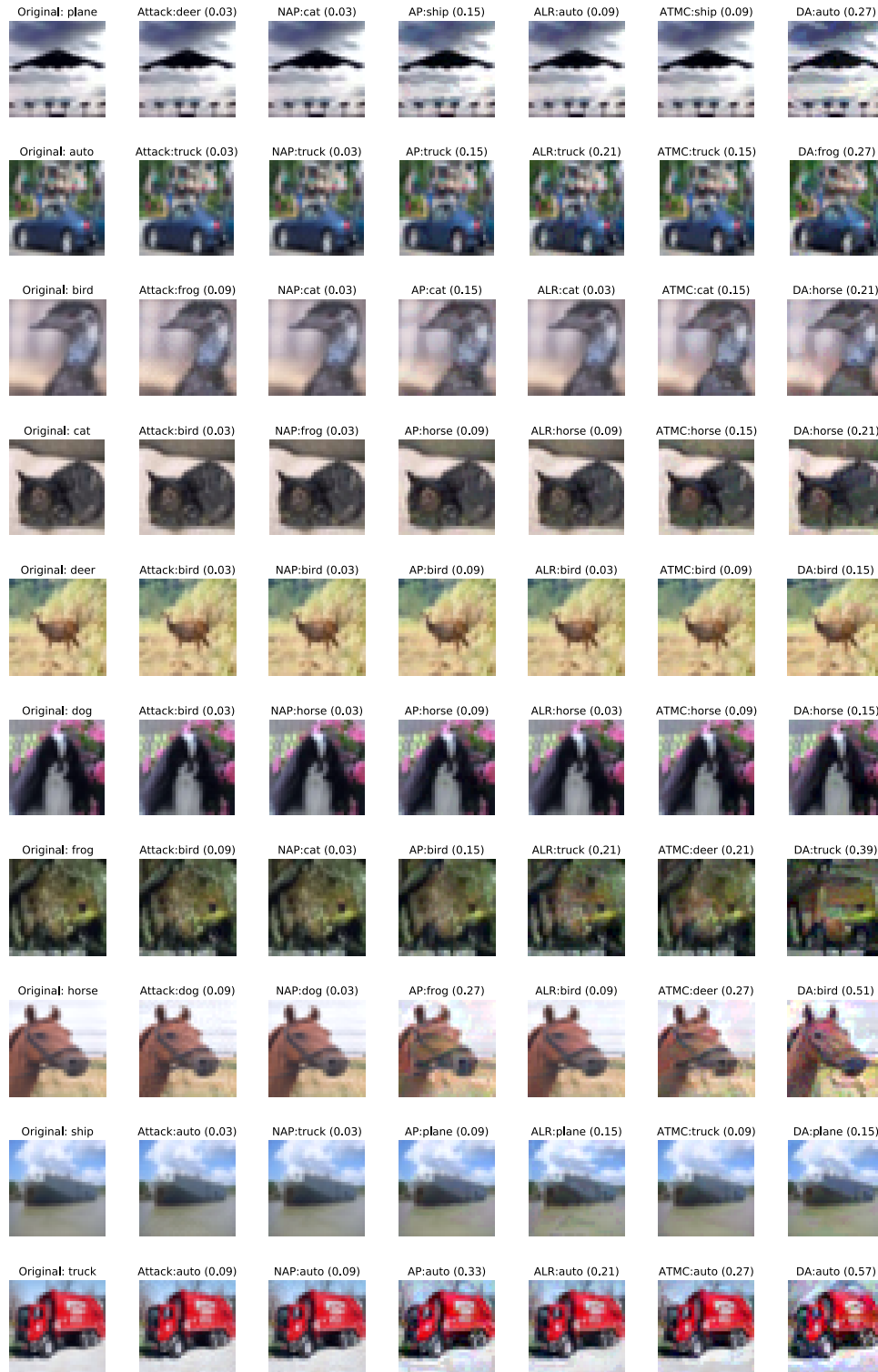


Figure 13: Visualization of the smallest magnitude adversarial perturbations found to fool models on CIFAR-10 dataset

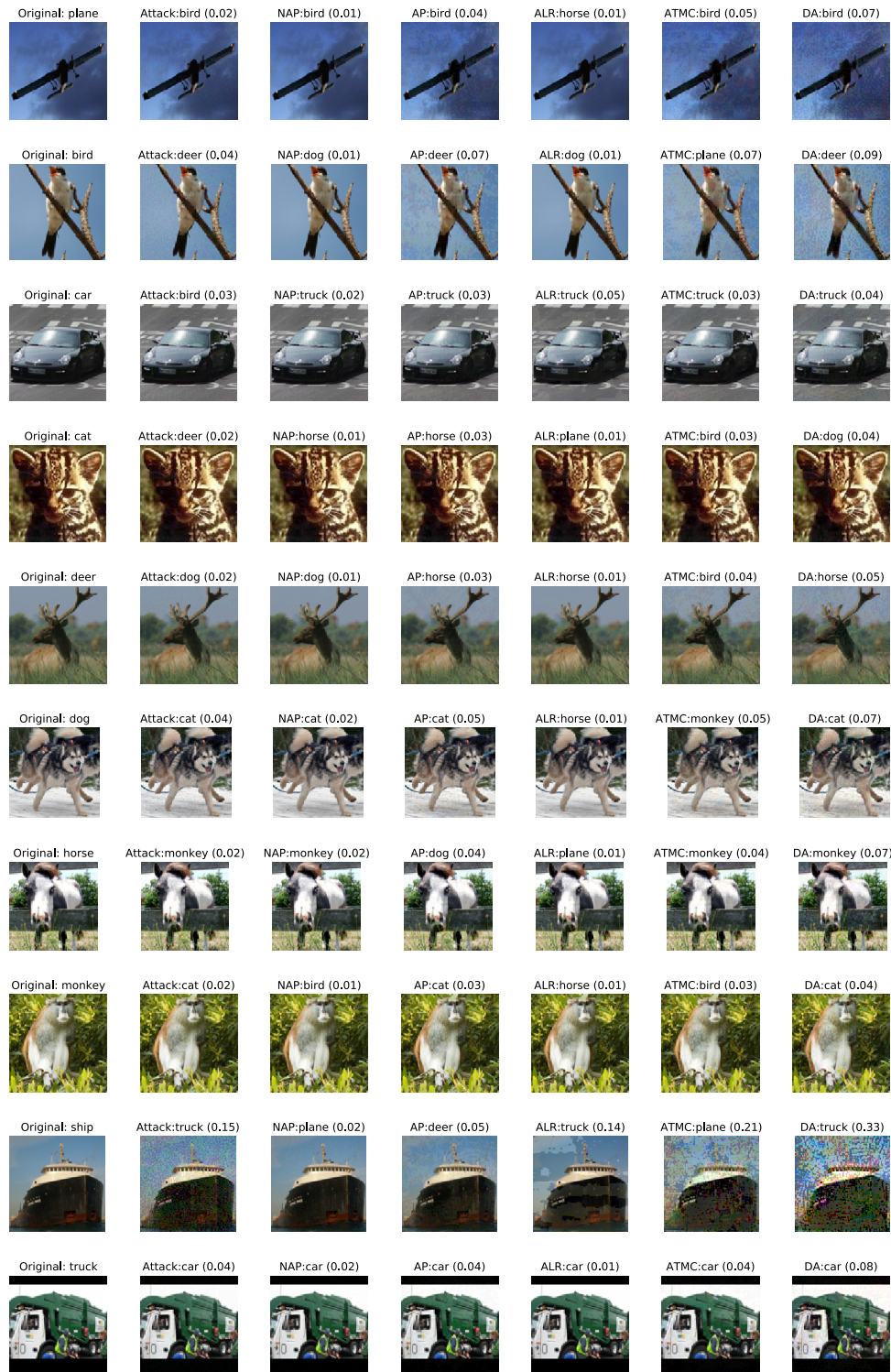


Figure 14: Visualization of the smallest magnitude adversarial perturbations found to fool models on STL-10 dataset

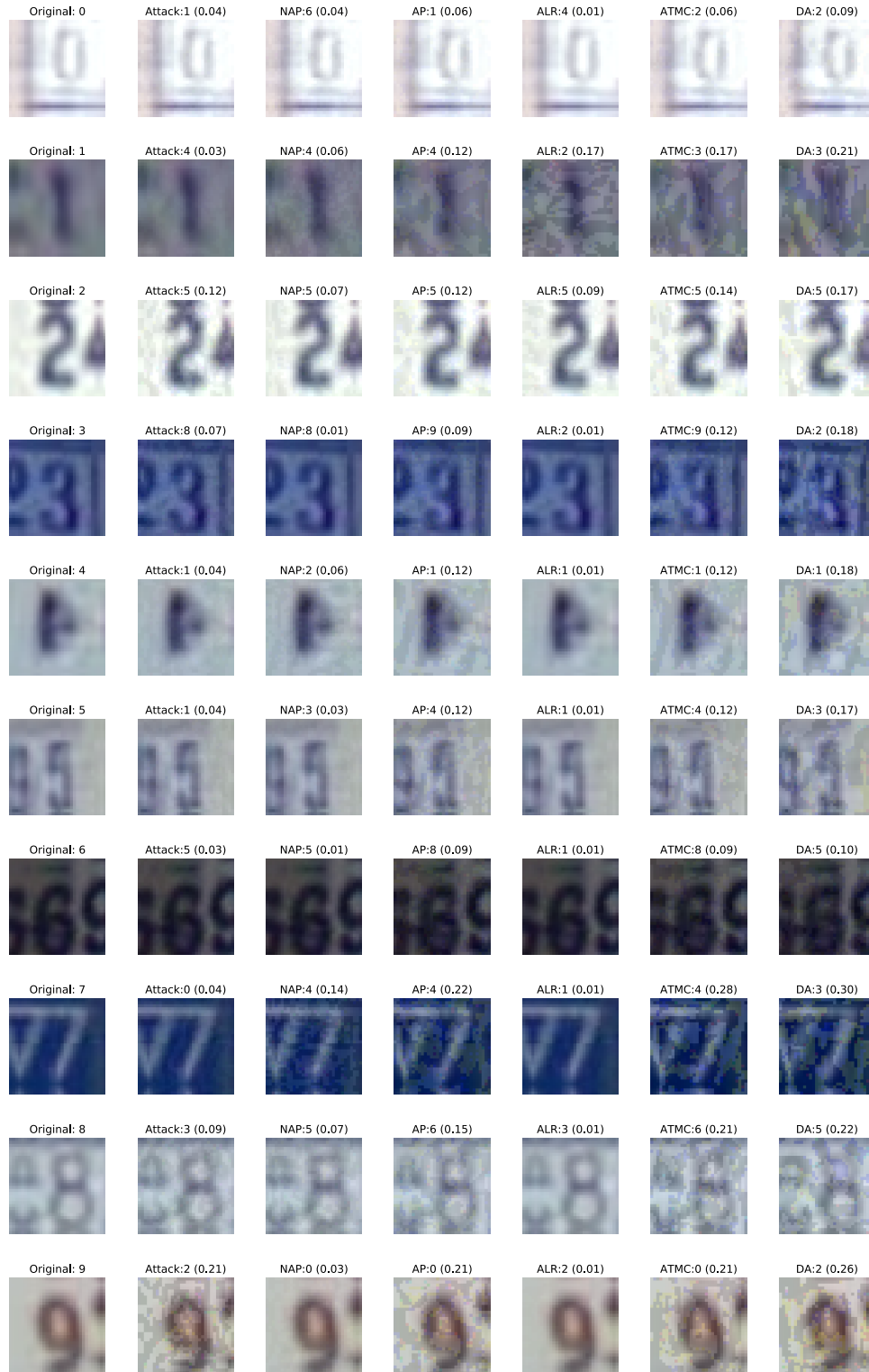


Figure 15: Visualization of the smallest magnitude adversarial perturbations found to fool models on SVHN dataset